Electronic Supplementary Information

Precise Patterning of Single Crystal Arrays of Organic Semiconductors by Patterned Microchannel Dip-coating Method for Organic Field-Effect Transistors

Chaoqiang Wang,[#a] Zhengjun Lu,[#a] Wei Deng,[a] Wanqin Zhao,[a] Bei Lu,[a] Jie Xiao,[b] Xiujuan Zhang,[a] Jiansheng Jie[a] and Xiaohong Zhang*[a]*

[a] Institute of Functional Nano & Soft Materials (FUNSOM), Jiangsu Key Laboratory for Carbon-Based Functional Materials & Devices, Soochow University, Suzhou, Jiangsu 215123, P. R. China

[b] School of Chemical and Environmental Engineering, College of Chemistry, Chemical Engineering and Materials Science, Soochow University, Suzhou, Jiangsu 215123, P. R. China

E-mail: *xiaohong_zhang@suda.edu.cn, xjzhang@suda.edu.cn*

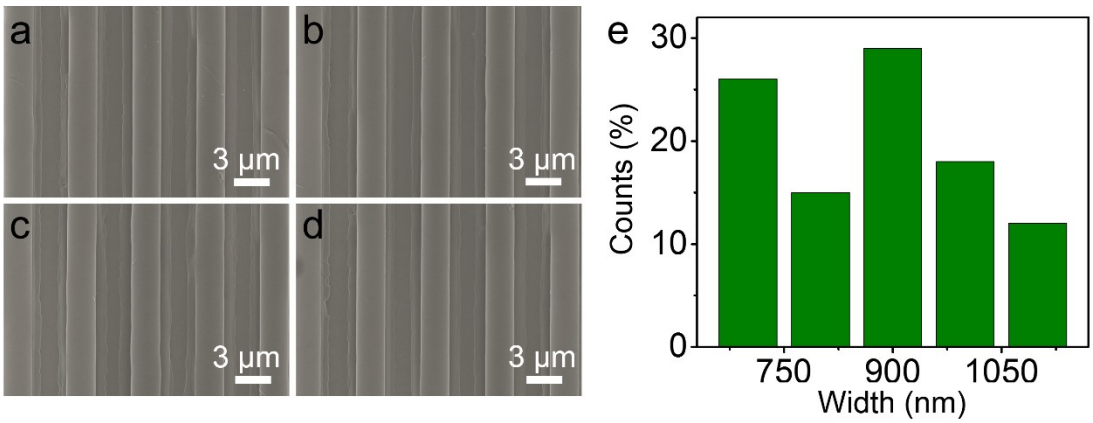

Fig. S1. (a-d) Typical SEM images the Dif-TES-ADT crystals in the patterned microchannels, (e) corresponding histogram of the crystal widths.

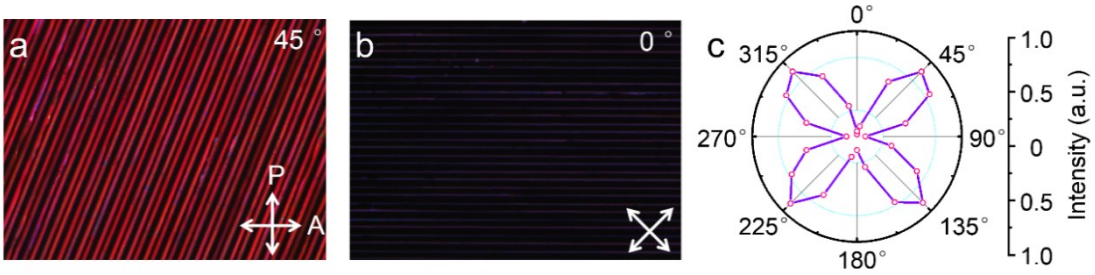

Fig. S2. (a, b) CPOM images and (c) normalized intensity of the pattern of the Dif-TES-ADT crystal arrays at different rotation angle.

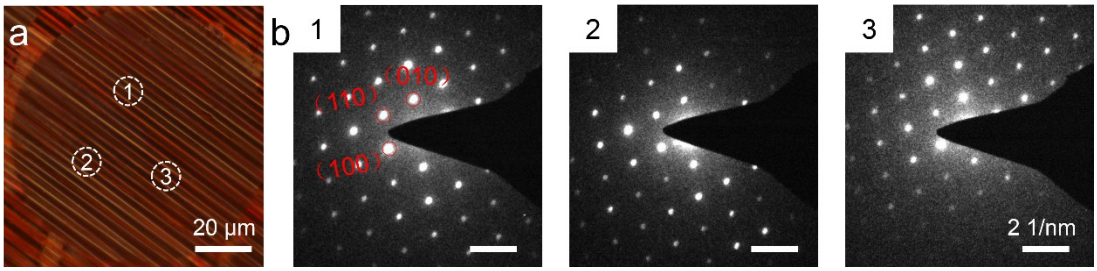

Fig. S3. (a) CPOM image of the pattern of Dif-TES-ADT crystal arrays on a Cu grid and (b) corresponding SAED patterns randomly selected from three different positions marked in (a).

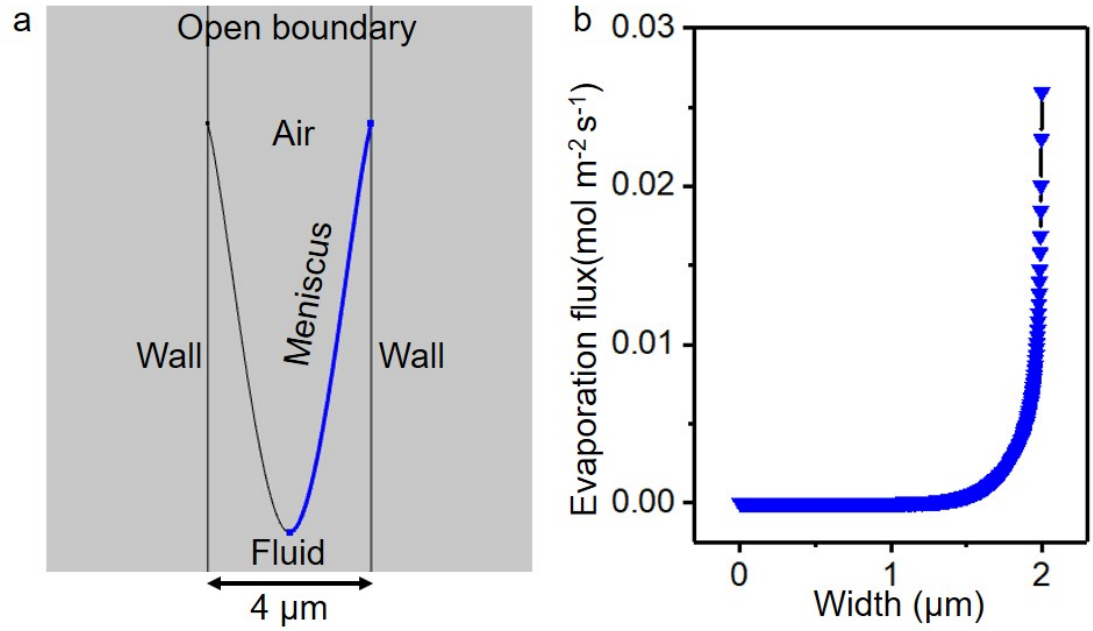

Fig. S4. (a) Geometry model of simulation (b) Evaporation flux along one side of meniscus.

Boundary conditions:

In the fluid domain, a non-slip condition was applied to the walls and a slip condition was set to the meniscus. Considering heat transfer in the fluid, amibent temperature condition was set to the walls. On the meniscus, a boundary heat source was implemented to represent the evaporation heat loss, which could be described as:

$JL = -k\nabla T \cdot n$

where J is the evaporation flux (mol m^{-2} s^{-1}), L representes latent heat (J mol^{-1}), k represents thermal conductivity (W m^{-1} K^{-1}) and **n** is the unit normal vector.

In the air domain, the concentration at the open boundary was set to 0 (mol m^{-3}), and the vapour concentration c_{sat} (mol m^{-3}) at the meniscus was determined by the saturated pressure:

$$c_{sat} = \frac{P_{sat}(T)}{RT}$$

The vapour pressure P_{sat} (Pa) was calculated from the Antoine equation:

$$log_{10}P_{sat} = A - \frac{B}{C+T}$$

where A = 7.0803, B = 1138.91, C = -41.69.[1]

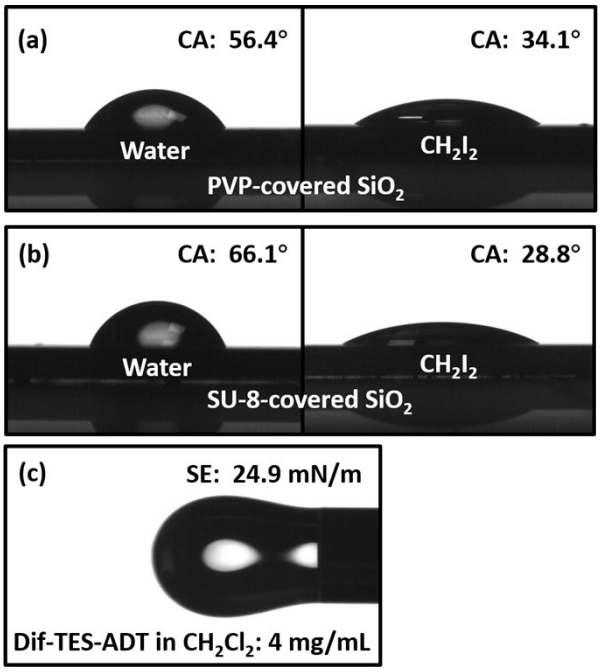

Fig. S5. (a,b) The contact angle of PVP and SU-8-covered SiO_2 substrates with two different test liquids of water and CH_2Cl_2, respectively. (c) The value of extracted surface tension of Dif-TES-ADT solution with concentration of 4 mg mL^{-1} in CH_2Cl_2.

DataPhysics OCA was adapt to assess the CA of substrates and surface tension (SE) of solution. The contact angle (CA) measurements were carried out *via* Owens and Wendt method[2,3] with two different test liquids of water and CH_2Cl_2 to evaluate the surface energy of PR and PVP-covered SiO_2 substrates. As shown in Fig. S9, the average CA measured with water and CH_2Cl_2 are 56.4° and 34.1° for PVP-covered substrates, whereas 66.1° and 28.8° for PR-covered substrates, respectively. We obtained the surface energy of SU-8 and PVP are of 49.14 mN/m and 51.96 mN/m , respectively. The value of extracted surface tension of Dif-TES-ADT solution with concentration of 4 mg mL^{-1} in CH_2Cl_2 is 24.93 mN/m.

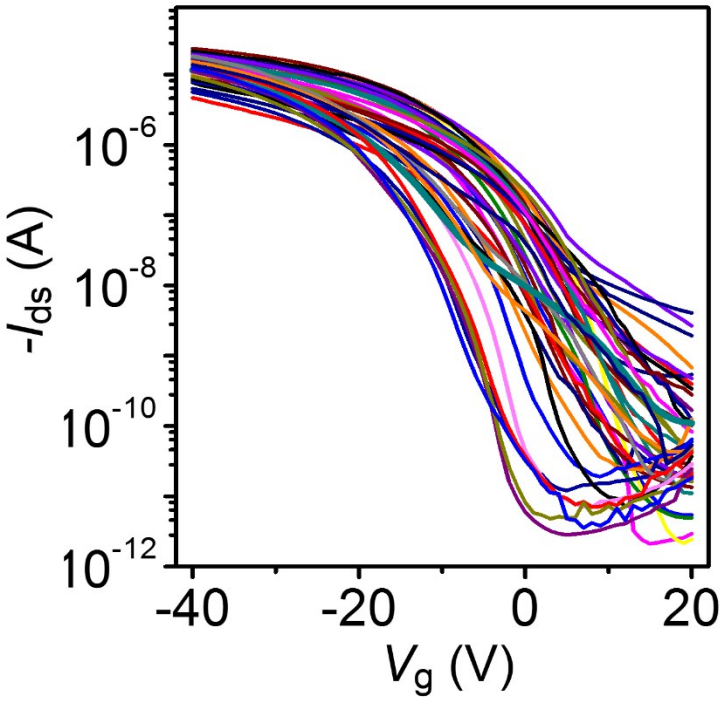

Fig. S6. Transfer characteristics of all the discrete OFETs on the same substrate.

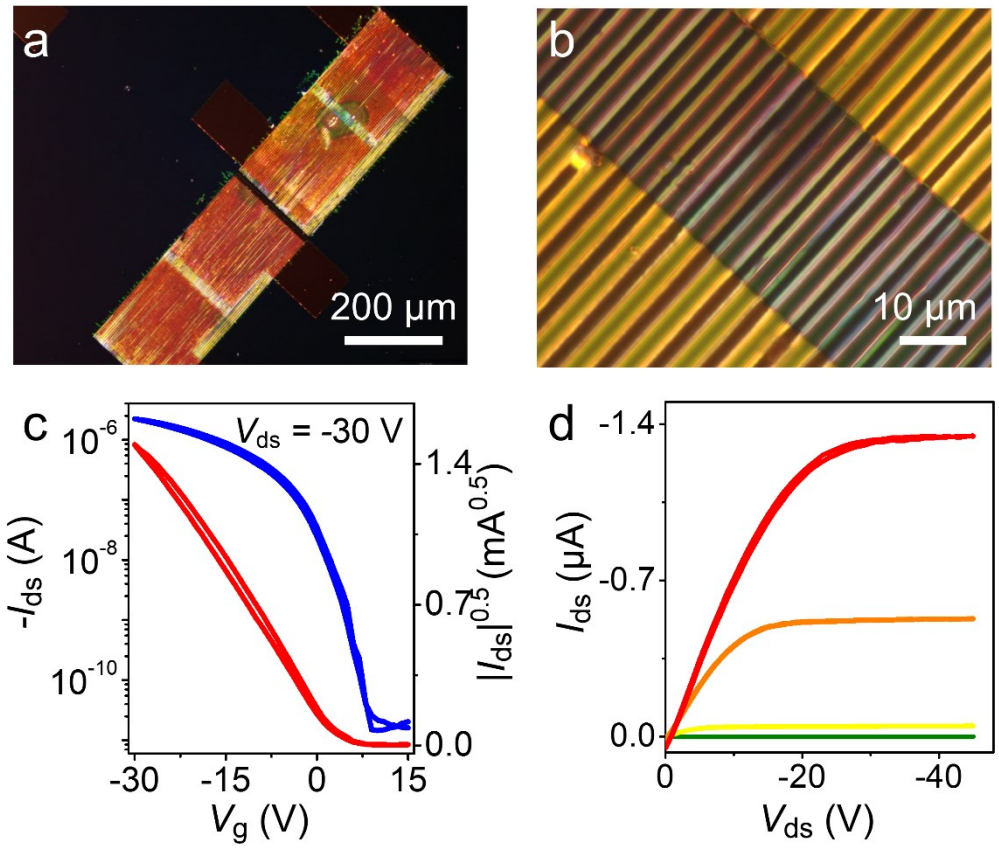

Fig. S7. (a,b) CPOM image of the pattern of Dif-TES-ADT crystal array deposited on the OFET channels. (c) Transfer and (d) output characteristics of the device.

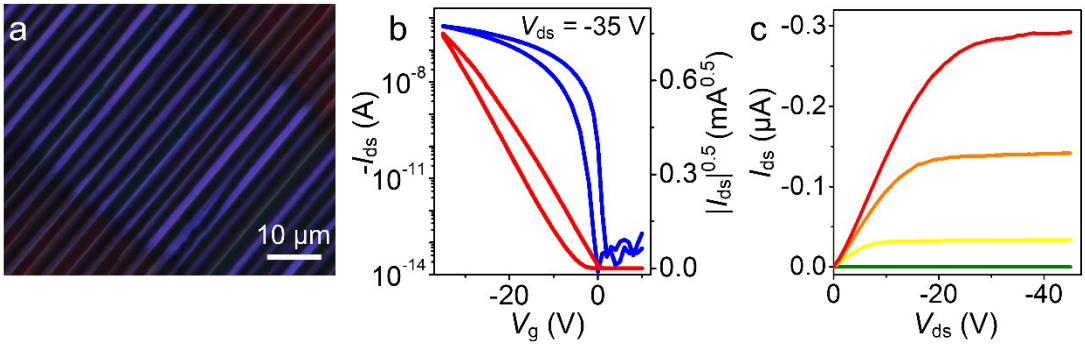

Fig. S8. (a) CPOM image of the pattern of TIPS-pentacene crystal array-based OFETs.

(b) Transfer and (c) output characteristics of the OFET.

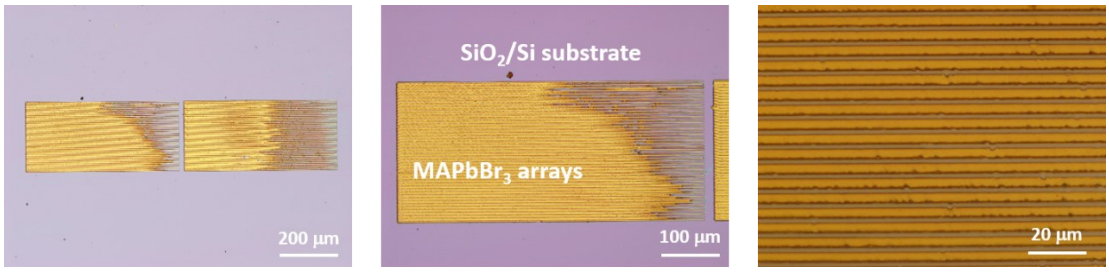

Fig. S9. The optical microscope images of $MAPbBr_3$ arrays grown by PMDC method.

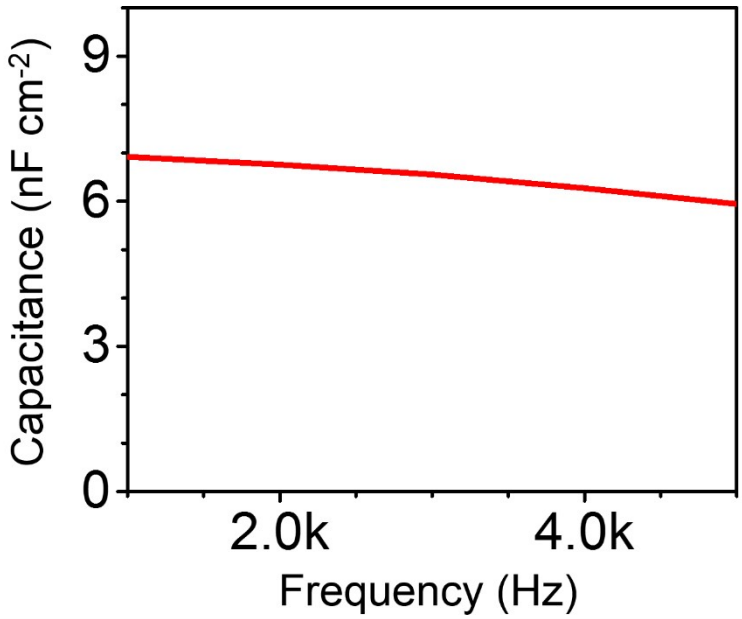

Fig. S10. Frequency dependence of capacitance for PVP dielectric layer at room temperature. The frequency dependence of capacitance for PVP dielectric was measured from the sandwich structure (Ag/PVP/SiO_2/Si), showing a capacitance of 6.92 nF cm^{-2} with electrode areas of 1 cm^2.

Table S1. Comparison of the different methods for patterning OSSCs.

Patterning Method	**Structure**	**Crystal orientation**	**Crystal location**	**Average mobility ($cm^2 V^{-1} s^{-1}$)**	**Ref.**
PDMC	**Single crystal**	**Controllable**	**Controllable**	**1.5**	**This work**
Inkjet printing	Polycrystal	Uncontrollable	Controllable	0.12-16.4	4-8
Channel-restricted meniscus self-assembly	Single crystal	Controllable	Uncontrollable	30.3	9
Vapor phase	Polycrystal	Uncontrollable	Controllable	-	10
Solution phase	Polycrystal	Uncontrollable	Controllable	0.038	11,12
Solution shearing	Polycrystal	Uncontrollable	Controllable	1.68	13
Photolithography-assisted spin-coating	Single crystal	Uncontrollable	Controllable	2.52	14
Surface-energy-controlled stepwise crystallization	Single crystal	Controllable	Uncontrollable	6	15
Capillary-assisted alternating-electric field	Single crystal	Uncontrollable	Controllable	-	16

References:

[1] C. L. Yaws and H. C. Yang, *Hydrocarbon Processing*, 1989, **68**, 65.

[2] D. K. Owens and R. C. Wendt, *Jour. of Applied Polymer Science*, **1969**, 13, 1741-1747.

[3] R. J. Good and L. A. Girifalco, *J. Phys. Chem.*, **1960**, 64, 561-565.

[4] S. H. Lee , M. H. Choi, S. H. Han, D. J. Choo, J. Jang, S. K. Kwon, *Org. Electron.*, **2008,** 9, 721-726.

[5] B. K. C. Kjellander, W. T. T. Smaal, K. Myny, J. Genoe, W. Dehaene, P. Heremans, G. H. Gelinck, *Org. Electron*., **2013**, 14, 768-774.

[6] J. A. Lim, W. H. Lee, H. S. Lee, J. H. Lee, Y. D. Park, K. Cho, *Adv. Funct. Mater.,* **2008**, 18, 229-234.

[7] Y. Kim, B. Yoo, J. E. Anthony, S. K. Park, *Adv. Mater.*, **2012**, 24, 497-502.

[8] H. Minemawari, T. Yamada, H. Matsui, J. Tsutsumi, S. Haas, R. Chiba, R. Kumai, T. Hasegawa, *Nature*, **2011**, 475, 364-367.

[9] W. Deng, X. Zhang, H. Dong, J. Jie, X. Xu, J. Liu, L. He, L. Xu, W. Hu, X. Zhang, Mater. Today, 2019, 24, 17-25.

[10] S. C. B. Mannsfeld, A. L. Briseno, S. Liu, C. Reese, M. E. Roberts, Z. Bao, *Adv. Funct. Mater.* ,**2007**, 17, 3545-3553.

[11] S. C. B. Mannsfeld, A. Sharei, S. Liu, M. E. Roberts, I. McCulloch, M. Heeney, Z. Bao, *Adv. Mater.*,**2008**, 20, 4044-4048.

[12] O. Goto, S. Tomiya, Y. Murakami, A. Shinozaki, A. Toda, J. Kasahara, D. Hobara, *Adv. Mater.*, **2012**, 24, 1117-1122.

[13] G. Giri , S. Park , M. Vosgueritchian , M. M. Shulaker, Z. Bao, *Adv. Mater.*, **2014**, 26, 487-493.

[14] W. Deng, X. Zhang, L. Wang, J. Wang, Q. Shang, X. Zhang, L. Huang, J. Jie, *Adv. Mater.*, **2015**, 27, 7305-7312.

[15] X. Zhang, J. Mao, W. Deng, X. Xu, L. Huang, X. Zhang, S. Lee, J. Jie, *Adv. Mater.*, **2018**, 30, 1800187.

[16] Y. Zhang, J. Jie, Y. Sun, S. Jeon, X. Zhang, G. Dai, C. J. Lee, X. Zhang, *Small*, **2017**, 13, 160426.